

UC Davis

UC Davis Previously Published Works

Title

The genome of the stress-tolerant wild tomato species *Solanum pennellii*

Permalink

<https://escholarship.org/uc/item/9fg9n2kt>

Journal

Nature Genetics, 46(9)

ISSN

1061-4036

Authors

Bolger, Anthony
Scossa, Federico
Bolger, Marie E
et al.

Publication Date

2014-09-01

DOI

10.1038/ng.3046

Peer reviewed

The genome of the stress-tolerant wild tomato species *Solanum pennellii*

Anthony Bolger^{1,2}, Federico Scossa^{3,4}, Marie E Bolger^{1,5}, Christa Lanz⁶, Florian Maumus⁷, Takayuki Tohge³, Hadi Quesneville⁷, Saleh Alseekh³, Iben Sørensen⁸, Gabriel Lichtenstein⁹, Eric A Fich⁸, Mariana Conte⁹, Heike Keller⁶, Korbinian Schneeberger^{6,10}, Rainer Schwacke^{1,5}, Itai Ofner¹¹, Julia Vrebalov¹², Yimin Xu¹², Sonia Osorio^{3,13}, Saulo Alves Aflitos¹⁴, Elio Schijlen¹⁴, José M Jiménez-Gómez^{15,16}, Malgorzata Rynhajllo¹, Seisuke Kimura¹⁷, Ravi Kumar¹⁷, Daniel Koenig^{6,17}, Lauren R Headland¹⁷, Julin N Maloof¹⁷, Neelima Sinha¹⁷, Roeland C H J van Ham^{14,21}, René Klein Lankhorst¹⁴, Linyong Mao¹², Alexander Vogel², Borjana Arsova¹⁸, Ralph Panstruga¹⁹, Zhangjun Fei^{12,20}, Jocelyn K C Rose⁸, Dani Zamir¹¹, Fernando Carrari⁹, James J Giovannoni^{12,20}, Detlef Weigel⁶, Björn Usadel^{1,2,5} & Alisdair R Fernie³

Solanum pennellii is a wild tomato species endemic to Andean regions in South America, where it has evolved to thrive in arid habitats. Because of its extreme stress tolerance and unusual morphology, it is an important donor of germplasm for the cultivated tomato *Solanum lycopersicum*¹. Introgression lines (ILs) in which large genomic regions of *S. lycopersicum* are replaced with the corresponding segments from *S. pennellii* can show remarkably superior agronomic performance². Here we describe a high-quality genome assembly of the parents of the IL population. By anchoring the *S. pennellii* genome to the genetic map, we define candidate genes for stress tolerance and provide evidence that transposable elements had a role in the evolution of these traits. Our work paves a path toward further tomato improvement and for deciphering the mechanisms underlying the myriad other agronomic traits that can be improved with *S. pennellii* germplasm.

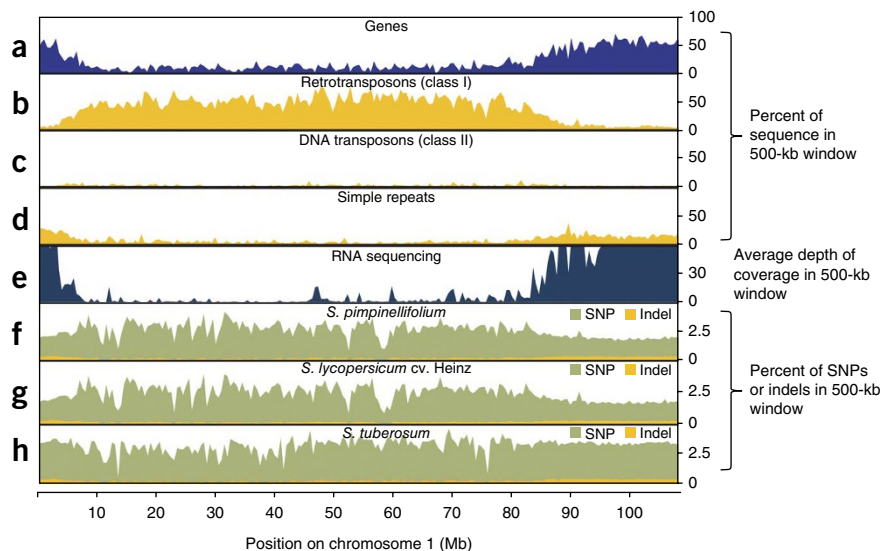
Crosses between distantly related plants can lead to substantial improvements in performance. Notably, *S. pennellii* × *S. lycopersicum* ILs have been used to define numerous quantitative trait loci (QTLs) for superior yield, chemical composition, morphology, abiotic stress

tolerance and extreme heterosis^{3,4}. Although genetic studies have proven informative, few genes underlying specific QTLs have been cloned, largely because of the lack of a *S. pennellii* genome sequence. To support QTL analyses, we sequenced the genome of *S. pennellii* using Illumina sequencing with ~190-fold coverage (Fig. 1 and Supplementary Tables 1–5). The initial assembly size was 942 Mb, with a scaffold N50 value of 1.7 Mb and N90 value of 0.43 Mb (Table 1 and Supplementary Tables 6 and 7). We estimated the total genome size to be about 1.2 Gb using a *k*-mer-based analysis (Supplementary Fig. 1 and Supplementary Table 8), in accordance with previous estimations^{3,4}. We anchored 97.1% of the genome assembly to chromosomes using genetic maps and restriction site-associated DNA sequencing (RAD-seq)-based markers from the IL population⁵ (Supplementary Note). Comparison of the assembly to publicly available BAC sequences indicated an accuracy of >99.9%, and a satisfactory accuracy of gap-filled regions was shown by realigning reads (Supplementary Fig. 2 and Supplementary Table 9). Of the 307,350 *S. lycopersicum* and 7,812 *S. pennellii* publicly available ESTs, 93% and >96% could be aligned to the genome, respectively (Supplementary Table 10), indicating comprehensive coverage of the gene-rich regions. We predicted 32,273 high-confidence genes and a potential set of 44,966 protein-coding genes and checked these

¹Department of Metabolic Networks, Max Planck Institute of Molecular Plant Physiology, Potsdam-Golm, Germany. ²Institute for Biology I, Institute for Botany and Molecular Genetics (IBMG), RWTH Aachen University, Aachen, Germany. ³Department of Molecular Physiology, Max Planck Institute of Molecular Plant Physiology, Potsdam-Golm, Germany. ⁴Consiglio per la Ricerca e la Sperimentazione in Agricoltura, Centro di Ricerca per l'Orticoltura, Pontecagnano, Italy. ⁵Institut für Bio- und Geowissenschaften 2 (IBG-2) Plant Sciences, Forschungszentrum Jülich, Jülich, Germany. ⁶Department of Molecular Biology, Max Planck Institute for Developmental Biology, Tübingen, Germany. ⁷French National Institute for Agricultural Research (INRA), UR1164 Research Unit in Genomics Info (URGI), INRA de Versailles-Grignon, Versailles, France. ⁸Department of Plant Biology, Cornell University, Ithaca, New York, USA. ⁹Instituto de Biotecnología, Centro de Investigación en Ciencias Veterinarias y Agronómicas (CICVyA)–Instituto Nacional de Tecnología Agropecuaria (INTA) and Consejo Nacional de Investigaciones Científicas y Técnicas (CONICET), Castelar, Argentina. ¹⁰Department of Plant Developmental Biology, Max Planck Institute for Plant Breeding Research, Cologne, Germany. ¹¹Faculty of Agriculture, Hebrew University of Jerusalem, Rehovot, Israel. ¹²Boyce Thompson Institute for Plant Research, Cornell University, Ithaca, New York, USA. ¹³Instituto de Hortofruticultura Subtropical y Mediterránea 'La Mayora', Department of Molecular Biology and Biochemistry, University of Málaga, Málaga, Spain. ¹⁴Plant Research International, Wageningen University and Research Centre, Wageningen, the Netherlands. ¹⁵Department of Plant Breeding and Genetics, Max Planck Institute for Plant Breeding Research, Cologne, Germany. ¹⁶INRA, UMR 1318, Institut Jean-Pierre Bourgin, Versailles, France. ¹⁷Department of Plant Biology, University of California, Davis, Davis, California, USA. ¹⁸Entwicklungs und Molekularbiologie der Pflanzen, Heinrich Heine Universität, Düsseldorf, Germany. ¹⁹Institute for Biology I, Unit of Plant Molecular Cell Biology, RWTH Aachen University, Aachen, Germany. ²⁰US Department of Agriculture Robert W. Holley Centre for Agriculture and Health, Ithaca, New York, USA. ²¹Present address: Keygene, Wageningen, the Netherlands. Correspondence should be addressed to B.U. (usadel@bio1.rwth-aachen.de).

Received 10 March; accepted 30 June; published online 27 July 2014; doi:10.1038/ng.3046

Figure 1 Genomic landscape of *S. pennellii* chromosome 1. (a–d) Densities of genes (a), retrotransposons (b), DNA transposons (c) and simple repeats (d) are shown for a 500-kb window. (e) Average RNA sequencing coverage in a 500-kb window. (f–h) Percentages of variants relative to *S. pimpinellifolium* (f), *S. lycopersicum* (g) and *S. tuberosum* (h).



for codon usage (Supplementary Table 11). We found that 20,076 (ref. 6) protein-coding genes were functionally annotated and compared to other species (Supplementary Figs. 3–6, Supplementary Tables 12 and 13, and Supplementary Data Sets 1–6). The average gene had 5.7 exons and coded for a 518-amino-acid protein. Multiple statistical analyses indicated a complex interplay between *Copia* transposable elements and stress-related genes.

In addition, we sequenced the *S. lycopersicum* cv. M82 genome—the recurrent parent of the IL population—at approximately 44-fold coverage. We compared this sequence to the *S. lycopersicum* cv. Heinz genome⁷, identifying 1,338,510 variants, of which 1,188,524 were SNPs. There was a clear enrichment for variants on chromosomes 4, 5 and 11, likely as a result of putative *Solanum pimpinellifolium* introgressions into the M82 cultivar, as evidenced by pairwise SNP analyses (Supplementary Figs. 7–9). Previous analyses⁷ suggested introgression of *S. pimpinellifolium* into the Heinz cultivar genome, and our genome-wide data seem to suggest an additional introgression on chromosome 4 as well.

Almost 82% of the nongapped *S. pennellii* assembly consisted of repeats (Supplementary Fig. 10). Long terminal repeat (LTR)-retrotransposons (LTR-RT) elements were by far the most abundant repeats, comprising ~45% of the *S. pennellii* genome assembly. As in *S. lycopersicum*, there were many more *Gypsy*-type (349 Mb) than *Copia*-type (79 Mb) LTR-RTs in the *S. pennellii* genome (Supplementary Fig. 11). LTR-RTs have a substantial role in genome size variation, representing 355 Mb of the 781-Mb *S. lycopersicum* genome assembly and 428 Mb of 942 Mb in *S. pennellii*. We assessed the recent activity of LTR-RTs in these two tomato genomes and the potato (*Solanum tuberosum*) genome using a sequence alignment of full-length LTR-RTs and transformed distances into ages. This analysis showed that *S. pennellii* has a higher abundance of young LTR-RTs (~15% showed close to zero divergence; Supplementary Figs. 12 and 13) than *S. lycopersicum* (less than 5% showed very low divergence), which is especially pronounced for *Copia* elements. These results point toward different genome dynamics in these two species since their separation from a common ancestor.

We next compared orthologous gene pairs from *S. pennellii* and *S. lycopersicum* to find genes with evidence for positive selection (Supplementary Fig. 14, Supplementary Tables 14–17 and Supplementary Data Set 7), as indicated by a K_a/K_s ratio (ratio of

nonsynonymous to synonymous nucleotide changes) of >1.0. In the resulting gene list, we found an enrichment of genes encoding acyl-carrier proteins, which are known to be involved in lipid biosynthesis. This enrichment might reflect an adaptation of the *S. pennellii* hydrophobic cuticle to minimize transpiration water loss and thus promote survival in desert habitats.

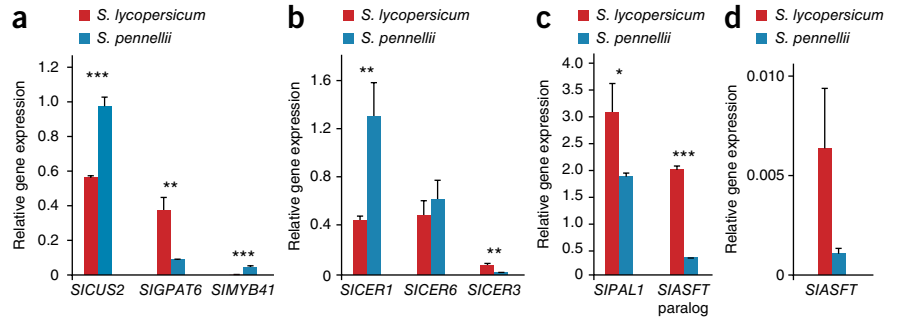
Previous studies on the fruit cuticles of wild tomato species documented considerable diversity in waxes and cutin⁸. We therefore analyzed the leaf cuticular waxes of both *S. pennellii* and *S. lycopersicum* and observed a threefold greater abundance of waxes, primarily very-long-chain alkanes, in *S. pennellii* (Supplementary Fig. 15). The alkane abundance in *S. pennellii* and the higher ratio of alkanes to triterpenoids have previously been suggested as mechanisms for increasing resistance to water flux across the cuticle^{9,10}. Additionally, the phenylpropanoid component of *S. pennellii* cutin was reduced to ~20% of that found in *S. lycopersicum*. We thus compared the expression of orthologs of known cuticle biosynthesis-related genes in the two species (Fig. 2, Supplementary Fig. 16 and Supplementary Tables 18 and 19). The expression of *CER1*, an ortholog of a key regulator of alkane concentrations in *Arabidopsis thaliana*¹¹, was substantially higher in *S. pennellii*, consistent with the greater abundance of alkanes. In contrast, a consistent differential expression pattern was not evident for genes associated with the biosynthesis of aliphatic cutin components, in agreement with the absence of major differences in cutin biochemical data. Lastly, the abundance of cutin phenylpropanoids in *S. lycopersicum* correlated with the much higher expression of two feruloyltransferase homologs and *PAL1*, which encodes the phenylpropanoid pathway gateway enzyme. This comparative analysis of the genome sequences of *S. pennellii* and *S. lycopersicum*, together with gene expression studies, demonstrates their potential for elucidating the ecological constraints and adaptations underlying traits of agronomic importance.

Table 1 *S. pennellii* genome assembly statistics

Stage	N50	N90	Contigs/scaffolds	$n > N50$	Assembled size (bp)	Unknown nucleotides	Anchored
Contigs	2,176	68	4,315,954	81,824	1,117,562,721	0	
Scaffolding	1,603,317	98,078	407,506	177	1,021,472,455	125,806,430	
Gap filling	1,590,935	95,443	407,506	177	1,012,612,203	67,624,937	
Final	1,741,129	437,042	4,579	156	942,595,034	67,190,021	97.1%

$n > N50$, number of sequences longer than the N50 length.

Figure 2 Expression of cuticle biosynthesis-related genes. (a–d) The expression of genes related to cutin biosynthesis (a) and wax biosynthesis (b) and of genes putatively (c) or known to be (d) associated with the formation of cuticular aromatic components was analyzed using quantitative PCR to validate data from RNA sequencing experiments and biochemical analysis. Statistical analysis was performed using a two-tailed *t* test. **P* < 0.05, ***P* < 0.01, ****P* < 0.001. Gene expression shown is relative to that for actin (*Solyc05g054480*). Error bars, s.e.m.; four biological replicates, each with three technical replicates.



The high stress tolerance of *S. pennellii*, which has also been shown in some ILs (Supplementary Tables 20 and 21), led us to investigate its underlying mechanism. Stress tolerance has frequently been associated with allelic polymorphisms¹², copy number variation¹³ and constitutive or inducible differential expression of numerous genes involved in regulatory or metabolic pathways¹⁴. To specifically target stress-related mechanisms, we identified 389 potential stress-related genes by mining the literature (Supplementary Table 22). These genes were filtered against drought- or salt-related QTLs detected in the ILs^{14–19}, which resulted in the identification of 100 candidate

genes (Fig. 3 and Supplementary Note). Alignment of the M82 and *S. pennellii* protein sequences indicated only minor differences, with no outliers in *K_a/K_s* ratios (Supplementary Data Set 7). Most non-synonymous changes, if any, occurred in the less-conserved portions of the protein sequences (Supplementary Note), with a few instances occurring in highly conserved portions of the protein sequences, as was the case for dehydration-responsive element-binding protein 1 (*DREB1*, *Solyc06g050520*)²⁰.

Further investigation showed that around half of the candidate stress-related genes had extensive polymorphisms in the regions upstream of their initiation codons. These sequence polymorphisms

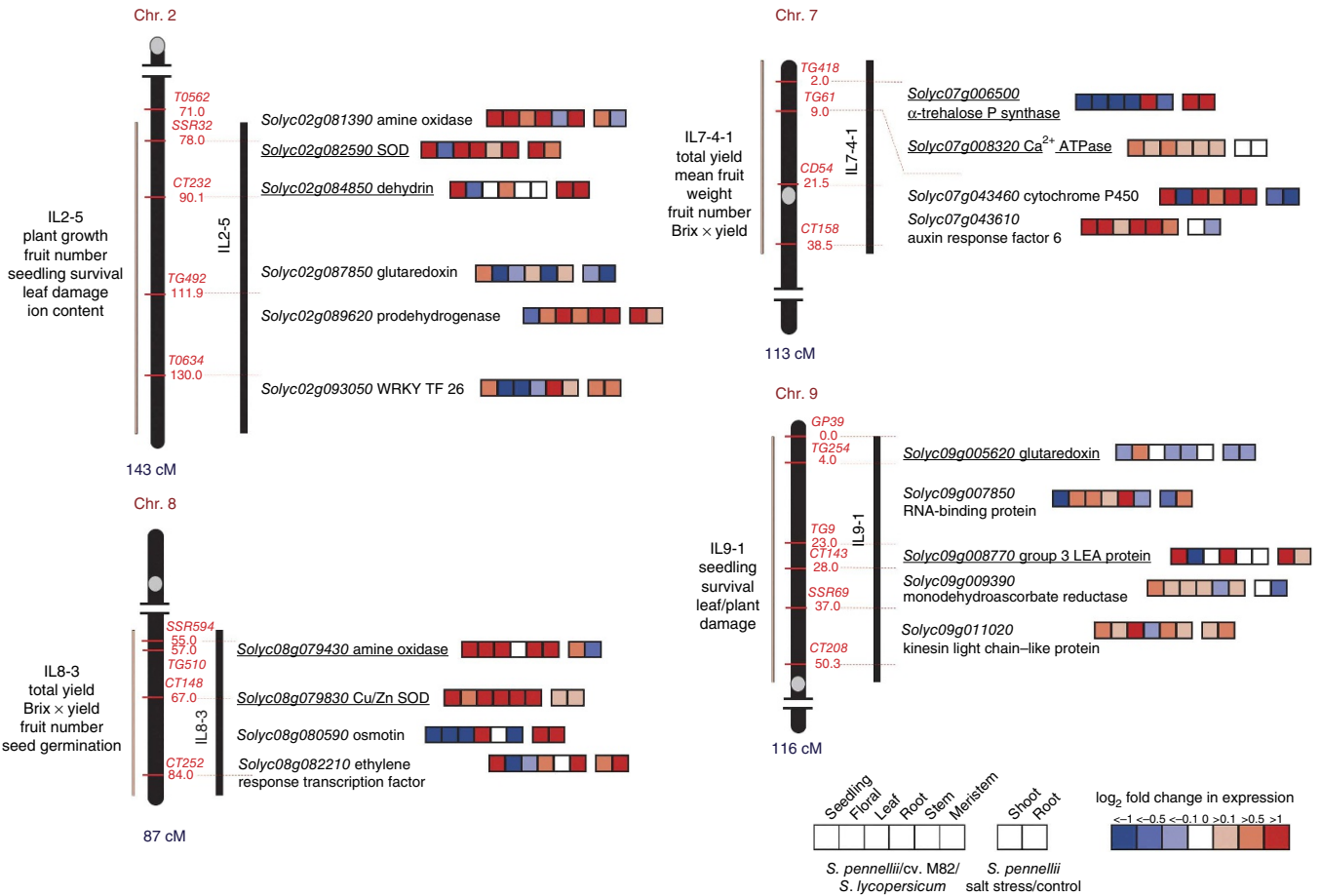


Figure 3 Chromosome mapping of stress-related candidate genes. Candidate genes related to salt stress and drought are visualized on their respective IL QTLs for selected ILs 2–5, 7–4–1, 8–3 and 9–1. Colored squares next to each gene represent the magnitude of differential expression (\log_2) across a range of different tissues and conditions. Red indicates higher expression in *S. pennellii*, and blue indicates higher expression in *S. lycopersicum*. Underlined genes are those characterized by large differences in expression between *S. lycopersicum* cv. M82 and *S. pennellii* at the promoter and/or coding sequence level. Large differences are characterized as large (>30-bp) indels in the promoter region and/or at least one significant amino acid change in the coding sequence as determined by the *P* value predicted by SIFT Blink⁴⁵. Brix × yield, total agronomic yield.

correlated with the magnitude of differential expression detected between M82 and *S. pennellii*²¹ (**Supplementary Tables 23 and 24**). One *S. pennellii* gene, a member of the drought tolerance–promoting dehydrin family (*Solyc02g084850*), contained two upstream insertions. A search for *cis*-acting elements in these two insertions showed the presence of several overlapping motifs, including some *cis* elements specifically responsive to dehydration (for example, MYCATRD22). This gene has been reported to show higher expression in the more drought-tolerant *S. pennellii* seedlings in comparison to M82 (ref. 21).

We further used the stress-related gene set to survey the colocalization of these genes with retrotransposons in the two species (**Supplementary Note and Supplementary Data Sets 8–12**). Stress-related genes (**Supplementary Table 25**) were found to be enriched in a 5-kb window around *Copia*-like retrotransposons in *S. pennellii* and *S. lycopersicum*. However, this enrichment was much more pronounced in *S. pennellii* ($P < 0.0001$ versus $P = 0.001$), and the enrichment around *Gypsy* elements was significant ($P = 0.0021$) in *S. pennellii* only (**Supplementary Fig. 17 and Supplementary Note**). Unsurprisingly, *Copia* elements in the proximal promoters (500 bp in length) of *S. pennellii* genes led to lower expression of these genes than for orthologous genes in *S. lycopersicum* that lacked such a *Copia* element, under standard conditions (**Supplementary Note**). We then investigated the correlation between the distribution of *Copia*-like elements and gene expression data from a published data set²² studying drought stress in leaves from *S. pennellii* and *S. lycopersicum*. We found a significant enrichment of *S. pennellii*-specific *Copia* elements within 5 kb of genes that were more stress responsive in *S. pennellii* than their *S. lycopersicum* orthologs (66 of 293 upregulated genes, $P < 0.038$ and 69 of 399 downregulated genes, $P < 0.022$). Genes that were more stress responsive in *S. lycopersicum* than their orthologs in *S. pennellii* were not significantly associated with *S. lycopersicum*-specific *Copia*-like elements (**Supplementary Note**).

This differential distribution of *Gypsy* and *Copia*-like elements, along with their association with stress responsiveness, suggests that, at least in some instances, LTR-RTs may exert a potential role in the regulation of gene expression. Such a role was proposed decades ago²³, and some evidence of a role for transposable elements in the modulation of proximal gene expression has accumulated^{24–26}. Our *S. pennellii* data set thus provide grounds, in future investigations, to assess the hypothesis that, in specific gene neighborhoods, *Copia*-like elements might represent ‘conditional’ regulatory sequences co-opted by the host genome upon exposure to different environmental stresses.

S. pennellii has additionally been widely documented to show phenotypes divergent from *S. lycopersicum* in relation to fruit development, maturation and metabolism^{27–33} (**Supplementary Note and Supplementary Data Set 13**). In terms of fruit maturation, several differences in the sequence and expression of some key regulatory genes were apparent. Most notable were differences in positive regulators, such as the *FUL1* MADS-box gene³⁴ that might be masked by the redundant *FUL2* gene, and reduced expression and predicted activity of *AP2A*³⁵, a negative regulator of ethylene synthesis that might compensate for the reduced ethylene production of maturing *S. pennellii* fruit³⁶.

Analyses of differential gene expression in mature fruit were dominated by photosynthesis-related genes, which showed considerably higher expression in *S. pennellii*, consistent with the lack of a chloroplast-to-chromoplast transition in this species. Elevated expression of *GLK2* (refs. 37,38) in *S. pennellii* fruit is consistent with these phenotypes.

Primary metabolism–associated genes did not show any unexpected changes in behavior, with core metabolic pathways having essentially conserved gene structures and similar expression patterns in the two species. Secondary metabolism in *S. pennellii* is considerably more complex, as evidenced by its glycoalkaloid, acyl sugar, terpene, carotenoid and volatile content. The additional glycoalkaloids in *S. pennellii* can be toxic, and their abundance is reflected in the relative expression of decorative enzymes of glycoalkaloid biosynthesis in *S. pennellii* and *S. lycopersicum*³⁹ (**Supplementary Note**), with similar patterns also observed for acyl sugars and terpenes^{29,33}. Variants seen in several carotenoid pathway genes, including *PSY1* and *lyc-B* genes, are consistent with the lack of lycopene accumulation in mature *S. pennellii* fruit (**Supplementary Note**). Domestication has selected against anti-nutrients and bitter-tasting flavors in *S. lycopersicum* but has also inadvertently led to poorer tasting tomatoes, which is in part a consequence of reduced volatile production^{40,41}. A detailed analysis showed divergence in both the sequence and expression of different volatile content–associated genes (**Supplementary Note**). A more complete understanding of these candidate genes, alongside those involved in the flavonoid and vitamin biosynthetic pathways, will likely greatly facilitate the breeding of better tasting and more nutritious fruit.

In conclusion, we have generated a valuable resource for the characterization of QTLs in the *S. pennellii* × *S. lycopersicum* IL population and have provided examples of how this genomics resource can be used to understand changes in response to water deficit, fruit maturation and metabolism. These investigations demonstrate the power of sequencing the parental lines of immortalized genetic populations for which a broad spectrum of phenotypic data has been collected⁴². One of the next challenges is to combine these phenotypic data with data gleaned from the genomes to explain the myriad of QTLs that have already been identified. For a comprehensive understanding of the evolutionary mechanism at play in the diverse *Solanum* genus, access to even more genomes is crucial.

Notably, this study suggests that the distinctive morphological characteristics of *S. pennellii* involved in differential stress resistance might be underpinned both by alterations in cuticle composition and nonrandom association of specific gene sets with transposable elements. Further investigations are needed to shed light on the role of candidate transposable elements in transcriptional rewiring and genome evolution^{43,44} within the tomato clade.

METHODS

Methods and any associated references are available in the [online version of the paper](#).

Accession codes. The *S. pennellii* (LA716) raw data have been deposited with the European Bioinformatics Institute (EBI) under project number [PRJEB5809](#). The genome sequence is available from the European Nucleotide Archive (ENA) under accessions [HG975439–HG975452](#). The *S. lycopersicum* cv. M82 raw data have been deposited at the EBI under project number [PRJEB6302](#). The genome sequence is available from the ENA under accessions [HG975512–HG975525](#).

Note: Any Supplementary Information and Source Data files are available in the online version of the paper.

ACKNOWLEDGMENTS

We gratefully acknowledge the support of the Max Planck Society in the form of an exceptional grant to cover the costs of sequencing the tomato species. In addition, work in the laboratories of D.Z. and A.R.F. was funded in the framework of Deutsche Israeli Project FE 552/12-1, which is administered by the Deutsche

Forschungsgemeinschaft. B.U. and M.E.B. acknowledge the support of the Bundesministerium für Bildung und Forschung (BMBF)-funded primary database FKZ 0315961. B.A. thanks the Deutsche Forschungsgemeinschaft International Research Training Groups (IRTG) 1525. F.S. acknowledges the support of the CRA Young Investigator Program. Work in the laboratory of F.C. was funded by INTA, Consejo Nacional de Investigaciones Científicas y Técnicas (CONICET) and Agencia Nacional de Promoción Científica y Tecnológica (ANPCYT) grants. Work in the laboratories of N.S. and J.N.M. was funded by NSF grant IOS-0820854. J.R. was supported by the US National Science Foundation (Plant Genome Program; DBI-0606595 and DBI-1313887) and by Agriculture and Food Research Initiative competitive grant 2011-04197 from the USDA National Institute of Food and Agriculture. Work in the laboratories of J.G. and Z.F. was additionally supported by US National Science Foundation Plant Genome Program grants DBI-0820612 and IOS-0923312. A.B. would like to thank Y. Brotman for preparing the *Pseudomonas syringae*-infected *S. pennellii* samples.

AUTHOR CONTRIBUTIONS

A.B., B.U. and A.R.F. managed the project. A.B., F.S., M.E.B., F.M., T.T., K.S., R.S., I.O., J.N.M., N.S., Z.F., J.K.C.R., D.Z., F.C., J.J.G., D.W., B.U. and A.R.F. designed the analysis. F.S., M.E.B., H.K., C.L., M.C., Y.X., S.A.A., M.R., B.U. and A.V. conducted DNA and RNA preparation and sequencing. C.L., J.M.J.-G., S.K., J.V., E.S., R.K., D.K., L.R.H., R.C.H.J.v.H., R.K.L., R.P., D.W. contributed new reagents and analytical tools. A.B., F.S., G.L., F.M., R.S., B.U. and A.R.F. conducted the data analyses. H.Q., S.A., I.S., E.A.F., S.O., L.M. and B.A. identified and evaluated candidate genes. B.U., A.B., M.E.B., F.S., D.W., F.M., J.K.C.R. and A.R.F. wrote the manuscript with help from all authors.

COMPETING FINANCIAL INTERESTS

The authors declare competing financial interests: details are available in the [online version of the paper](#).

Reprints and permissions information is available online at <http://www.nature.com/reprints/index.html>.



This work is licensed under a Creative Commons Attribution-NonCommercial-ShareAlike 3.0 Unported License. The images or other third party material in this article are included in the article's Creative Commons license, unless indicated otherwise in the credit line; if the material is not included under the Creative Commons license, users will need to obtain permission from the license holder to reproduce the material. To view a copy of this license, visit <http://creativecommons.org/licenses/by-nc-sa/3.0/>.

- Rick, C. & Tanksley, S. Genetic variation in *Solanum pennellii*: comparisons with two other sympatric tomato species. *Plant Syst. Evol.* **139**, 11–45 (1981).
- Gur, A. & Zamir, D. Unused natural variation can lift yield barriers in plant breeding. *PLoS Biol.* **2**, e245 (2004).
- Arumuganathan, K. & Earle, E.D. Nuclear DNA content of some important plant species. *Plant Mol. Biol. Rep.* **9**, 208–218 (1991).
- Kamenetzky, L. *et al.* Genomic analysis of wild tomato introgressions determining metabolism- and yield-associated traits. *Plant Physiol.* **152**, 1772–1786 (2010).
- Chitwood, D.H. *et al.* A quantitative genetic basis for leaf morphology in a set of precisely defined tomato introgression lines. *Plant Cell* **25**, 2465–2481 (2013).
- Lohse, M. *et al.* Mercator: a fast and simple web server for genome scale functional annotation of plant sequence data. *Plant Cell Environ.* **37**, 1250–1258 (2014).
- Tomato Genome Consortium. The tomato genome sequence provides insights into fleshy fruit evolution. *Nature* **485**, 635–641 (2012).
- Yeats, T.H. *et al.* The fruit cuticles of wild tomato species exhibit architectural and chemical diversity, providing a new model for studying the evolution of cuticle function. *Plant J.* **69**, 655–666 (2012).
- Parsons, E.P. *et al.* Fruit cuticle lipid composition and fruit post-harvest water loss in an advanced backcross generation of pepper (*Capsicum* sp.). *Physiol. Plant.* **146**, 15–25 (2012).
- Vogg, G. *et al.* Tomato fruit cuticular waxes and their effects on transpiration barrier properties: functional characterization of a mutant deficient in a very-long-chain fatty acid beta-ketoacyl-CoA synthase. *J. Exp. Bot.* **55**, 1401–1410 (2004).
- Bourdenx, B. *et al.* Overexpression of *Arabidopsis* ECERIFERUM1 promotes wax very-long-chain alkane biosynthesis and influences plant response to biotic and abiotic stresses. *Plant Physiol.* **156**, 29–45 (2011).
- Asins, M.J. *et al.* Two closely linked tomato HKT coding genes are positional candidates for the major tomato QTL involved in Na⁺/K⁺ homeostasis. *Plant Cell Environ.* **36**, 1171–1191 (2013).
- Maron, L.G. *et al.* Aluminum tolerance in maize is associated with higher MATE1 gene copy number. *Proc. Natl. Acad. Sci. USA* **110**, 5241–5246 (2013).
- Gong, P. *et al.* Transcriptional profiles of drought-responsive genes in modulating transcription signal transduction, and biochemical pathways in tomato. *J. Exp. Bot.* **61**, 3563–3575 (2010).
- Eshed, Y., Abu-Abied, M., Saranga, Y. & Zamir, D. Lycopersicon esculentum lines containing small overlapping introgressions from *L. pennellii*. *Theor. Appl. Genet.* **83**, 1027–1034 (1992).
- Frary, A. *et al.* Salt tolerance in *Solanum pennellii*: antioxidant response and related QTL. *BMC Plant Biol.* **10**, 58 (2010).
- Frary, A., Keles, D., Pinar, H., Gol, D. & Doganlar, S. NaCl tolerance in *Lycopersicon pennellii* introgression lines: QTL related to physiological responses. *Biol. Plant.* **55**, 461–468 (2011).
- Gur, A. *et al.* Yield quantitative trait loci from wild tomato are predominately expressed by the shoot. *Theor. Appl. Genet.* **122**, 405–420 (2011).
- Uozumi, A. *et al.* Tolerance to salt stress and blossom-end rot in an introgression line, IL8–3, of tomato. *Sci. Hortic. (Amsterdam)* **138**, 1–6 (2012).
- Lata, C. & Prasad, M. Role of DREBs in regulation of abiotic stress responses in plants. *J. Exp. Bot.* **62**, 4731–4748 (2011).
- Koenig, D. *et al.* Comparative transcriptomics reveals patterns of selection in domesticated and wild tomato. *Proc. Natl. Acad. Sci. USA* **110**, E2655–E2662 (2013).
- Filippis, I., Lopez-Cobollo, R., Abbott, J., Butcher, S. & Bishop, G.J. Using a periclinal chimera to unravel layer-specific gene expression in plants. *Plant J.* **75**, 1039–1049 (2013).
- McClintock, B. Chromosome organization and genic expression. *Cold Spring Harb. Symp. Quant. Biol.* **16**, 13–47 (1951).
- Butelli, E. *et al.* Retrotransposons control fruit-specific, cold-dependent accumulation of anthocyanins in blood oranges. *Plant Cell* **24**, 1242–1255 (2012).
- Naito, K. *et al.* Unexpected consequences of a sudden and massive transposon amplification on rice gene expression. *Nature* **461**, 1130–1134 (2009).
- Quadrana, L. *et al.* Natural occurring epialleles determine vitamin E accumulation in tomato fruits. *Nat. Commun.* **5**, 4027 (2014).
- Schauer, N. *et al.* Comprehensive metabolic profiling and phenotyping of interspecific introgression lines for tomato improvement. *Nat. Biotechnol.* **24**, 447–454 (2006).
- Schauer, N. *et al.* Mode of inheritance of primary metabolic traits in tomato. *Plant Cell* **20**, 509–523 (2008).
- Schillmiller, A.L. *et al.* Monoterpenes in the glandular trichomes of tomato are synthesized from a neryl diphosphate precursor rather than geranyl diphosphate. *Proc. Natl. Acad. Sci. USA* **106**, 10865–10870 (2009).
- Tieman, D. *et al.* Functional analysis of a tomato salicylic acid methyl transferase and its role in synthesis of the flavor volatile methyl salicylate. *Plant J.* **62**, 113–123 (2010).
- Kochevenko, A. & Fernie, A.R. The genetic architecture of branched-chain amino acid accumulation in tomato fruits. *J. Exp. Bot.* **62**, 3895–3906 (2011).
- Mageroy, M.H., Tieman, D.M., Floystad, A., Taylor, M.G. & Klee, H.J. A *Solanum lycopersicum* catechol-O-methyltransferase involved in synthesis of the flavor molecule guaiaicol. *Plant J.* **69**, 1043–1051 (2012).
- Schillmiller, A.L., Charbonneau, A.L. & Last, R.L. Identification of a BAHD acetyltransferase that produces protective acyl sugars in tomato trichomes. *Proc. Natl. Acad. Sci. USA* **109**, 16377–16382 (2012).
- Bemer, M. *et al.* The Tomato FRUITFULL Homologs TDR4/FUL1 and MBP7/FUL2 regulate ethylene-independent aspects of fruit ripening. *Plant Cell* **24**, 4437–4451 (2012).
- Chung, M.Y. *et al.* A tomato (*Solanum lycopersicum*) APETALA2/ERF gene, SIAP2a, is a negative regulator of fruit ripening. *Plant J.* **64**, 936–947 (2010).
- Grumet, R., Fobes, J.F. & Herner, R.C. Ripening behavior of wild tomato species. *Plant Physiol.* **68**, 1428–1432 (1981).
- Nguyen, C.V. *et al.* Tomato GOLDEN2-LIKE transcription factors reveal molecular gradients that function during fruit development and ripening. *Plant Cell* **26**, 585–601 (2014).
- Powell, A.L. *et al.* Uniform ripening encodes a Golden 2-like transcription factor regulating tomato fruit chloroplast development. *Science* **336**, 1711–1715 (2012).
- Iijima, Y. *et al.* Steroidal glycoalkaloid profiling and structures of glycoalkaloids in wild tomato fruit. *Phytochemistry* **95**, 145–157 (2013).
- Tieman, D. *et al.* Tomato aromatic amino acid decarboxylases participate in synthesis of the flavor volatiles 2-phenylethanol and 2-phenylacetaldehyde. *Proc. Natl. Acad. Sci. USA* **103**, 8287–8292 (2006).
- Klee, H.J. Purple tomatoes: longer lasting, less disease, and better for you. *Curr. Biol.* **23**, R520–R521 (2013).
- Zamir, D. Where have all the crop phenotypes gone? *PLoS Biol.* **11**, e1001595 (2013).
- Bui, Q. & Grandbastien, M.-A. in *Plant Transposable Elements* Vol. 24 (eds. Grandbastien, M.-A. & Casacuberta, J.M.) 273–296 (Springer, Berlin, 2012).
- Lisch, D. How important are transposons for plant evolution? *Nat. Rev. Genet.* **14**, 49–61 (2013).
- Kumar, P. *et al.* Predicting the effects of coding non-synonymous variants on protein function using the SIFT algorithm. *Nat. Protoc.* **4**, 1073–1081 (2009).

ONLINE METHODS

The genome of *S. pennellii* LA0716 was sequenced using the whole-genome shotgun (WGS) approach on the Illumina platform. The three libraries of paired-end sequencing, with insert sizes of 205 bp, 275 bp and 515 bp, provided a total of 229.4 Gb of sequence data in 2.1 billion reads and were supplemented by 13 libraries of mate-pair sequencing, with insert sizes ranging from 3 kb to 40 kb, yielding an additional 348 million read pairs containing longer-distance structural information. Additionally, a BAC library was prepared and end sequenced using the Sanger approach.

Next-generation sequencing data were filtered to remove adaptors and low-quality base calls. Genome size estimation was performed using the *k*-mer counting approach (Supplementary Fig. 1). Filtered data were corrected, assembled, scaffolded and then gap filled. Contaminant scaffolds were detected by alignment of the assembly against the NCBI non-redundant nucleotide database, and scaffolds that were found to be closest to a reference sequence of non-plant origin were removed. Finally, the paired-end libraries were remapped to the assembly, and the resulting SNPs were used to correct the assembly.

Scaffolds were anchored to chromosome regions using a combination of traditional markers, BAC-end sequences and 'de novo' markers extracted from an existing RAD-seq data set of the *S. pennellii* IL population. Some scaffolds that were likely to have been misassembled were detected and split during this process. Nine existing BAC sequences were used to independently validate the genome.

The chloroplast was separately assembled by selecting for reads from very-high-coverage regions and assembling these, followed by manual arrangement to best align with the existing *S. lycopersicum* chloroplast sequence.

Gene annotation was performed using parameters trained for *S. lycopersicum*, supplemented by evidence from EST and RNA sequencing data. In addition to the publicly available EST and RNA sequencing data, 70 new RNA sequencing samples were sequenced covering a variety of conditions and tissues. The resulting gene transcripts were filtered on the basis of orthology against known related protein sequences and RNA support, at two different thresholds, resulting in a primary gene set and a high-confidence subset. These gene models were validated against the proteomes of *Arabidopsis*, *S. lycopersicum* and *S. tuberosum*.

Functional gene annotation and assignment to MapMan classes was performed using the Mercator pipeline. To enable cross-species comparison, the same pipeline version was used to annotate the *S. lycopersicum* and *S. tuberosum* gene models. MapMan classes that showed significant differences in their proportion in *S. pennellii* in comparison to the other species were further investigated manually. Orthology analysis was performed to identify simple orthologous pairs between *S. pennellii* and *S. lycopersicum* and also to identify orthologous gene families between *S. lycopersicum*, *S. tuberosum*, *Arabidopsis* and *Oryza sativa* (Supplementary Fig. 5).

Protein domains of *S. pennellii*, *S. lycopersicum* and *S. tuberosum* were analyzed using Interproscan and Pfam, identifying some notable differences.

Pectin esterase and P450 proteins (Supplementary Figs. 18–22) were aligned against the appropriate hidden Markov model (HMM), and phylogenetic trees were created. Evolutionary analysis was performed on orthologous gene pairs by first aligning their protein sequence and then calculating their K_a/K_s ratio.

The coding sequence, promoter sequence and expression of genes known to be involved in primary metabolism, secondary metabolism, fruit development and ripening were further investigated in *S. pennellii* and *S. lycopersicum*.

Expression patterns were compared by aligning RNA reads from six tissue types against the *S. pennellii* transcriptome (Supplementary Figs. 23 and 24, Supplementary Tables 26–29 and Supplementary Data Sets 14–16). The RPKM (reads per kilobase (of transcript) per million reads mapped) values from this analysis were hierarchically clustered with those available from *S. lycopersicum* and *S. pimpinellifolium*, using the pairwise orthologs described above.

Repeat analysis was performed by *de novo* identification of repeats followed by whole-genome annotation. Repeats were classified using the REPET classification utility followed by semi-manual curation. LTR insertion times were estimated by finding full-length LTR transposons, and sequence alignment and evolutionary distances were calculated and converted to ages using a previously established rate.

Various stress-related gene sets were tested for proximity to transposable elements. The initial investigation used a set of 389 genes manually identified from the literature, which were expanded using the gene family clusters to form a more statistically powerful gene set. This gene set was tested for enrichment around both *Gypsy* and *Copia* elements, using the Fisher's exact test. Further similar analyses were performed using salt stress-responsive genes in *S. pennellii*, as well as a cross-species comparison of drought-responsive genes between *S. pennellii* and *S. lycopersicum*.

The *S. lycopersicum* cv. M82 genome was resequenced using the existing *S. lycopersicum* cv. Heinz genome as a reference. One paired-end library was created with an insert size of 190 bp and sequenced to provide 574 million reads totaling 47.4 billion bases. These data were initially aligned to the Heinz reference genome, and this alignment was further refined. The detected variants were then applied to the genome, and a further round of alignment was performed, where additional SNPs were detected and applied to create the final M82 genome.

Waxes and cutin from *S. lycopersicum* cv. Heinz and *S. pennellii* leaves were extracted, derivatized and then analyzed by gas chromatography–mass spectrometry. Metabolic differences were cross-referenced with quantitative PCR-derived expression data for genes known to be involved in wax and cutin synthesis.

Detailed methods and their associated references can be found in the **Supplementary Note**.